Static Force Analysis of Mechanisms with Four-Bar Linkages Based on Flexibility Conditions

Sureyya Sahin Leila Notash

sahin@me.queensu.ca notash@me.queensu.ca

Department of Mechanical and Materials Engineering, Queen's University, Kingston, Ontario, Canada, K7L3N6

Fax: 1-613-533-6489

Abstract: The four-bar linkages are widely used in both planar and spatial mechanisms and robotic manipulators. Static force analysis of the four-bar mechanisms subjected to external loading working under gravitational forces is formulated in this article. The formulation is based on structural matrix force and stiffness methods with the free-body diagrams for each of the links considered. The four-bar mechanism considered is overdetermined as there are additional constraints compared to a statically determinate four-bar mechanism. A method of solution, based on the matrix force analysis, incorporating the flexibility of the mechanism is given. The methodology is simulated for a mechanism with a planar four-bar linkage where the plane of motion could be varied by rotating about a revolute joint that connects the four-bar linkage to the base.

1. Introduction

Four-bar mechanisms are of great importance in mechanism design since they are formed with the lowest number of links (bars) and they are one of the basic mechanisms used in obtaining more complex ones. For example, a widely used spatial four-bar mechanism consists of two spherical joints (S) and two revolute joints (R). This mechanism, which has a passive degree of freedom due to the spherical joint pair, can be used under spatial loading. The four-bar mechanisms, which have four revolute joints, are generally used for planar motion. The planar four-bar mechanism can be used spatially; however, the force analysis of the mechanism becomes overdetermined. To illustrate the problem, Grübler's equation for estimating the number of constraints, C, to be solved can be used:

$$C = \lambda \sum n - \sum_{i=1}^{j} f_i \tag{1}$$

where $\sum n$ is the total number of links, j is the total number of joints, and f_i is the degrees of freedom of joint i, and λ denotes the task space dimension, which is 3 for planar or spherical mechanisms and 6 for spatial mechanisms. Similarly, the number of force equations, E, can be calculated by:

$$E = \lambda (\sum n - 1) \tag{2}$$

Table 1 is prepared for the spatial and planar four-bar mechanisms and the planar four-bar mechanisms subjected to spatial loading. The equation for the idle degree of freedom in the spatial four-bar mechanism is eliminated in calculating the number of equations in Table 1 since it does not affect the motion of the mechanism as long as it is not actuated. The planar four-bar and spatial four-bar mechanisms are determined mechanisms whereas the planar four-bar becomes overdetermined when it is subjected to spatial loading. In most publications on four-bar mechanisms, the loading out of the plane of motion are either not given or neglected in the force analysis of the mechanism, or spatial four-bar mechanisms are used. However, the planar four-bars are used in the spatial mechanisms, e.g., in robotic manipulators [1, 2].

Table 1 The static determinacy of the four-bar mechanisms.

Mechanisms	Number of Constraints, C	Number or Equations, E	Minimum Number of Actuation
Planar four-bar (4R)	8	9	1
Planar four-bar - under spatial loading (4R)	20	18	1
Spatial four-bar (2R, 2S)	16	17	1

In this article, the static force analysis of a planar four-bar mechanism under spatial loading is considered. Although there are standard formulations of planar four-bar mechanisms under loading in the plane of the mechanism, or spatial four-bar mechanisms in spatial loading [3, 4], to the best of authors' knowledge there are not many studies for solving the planar four-bar mechanisms under spatial loading. The static force equations are written in matrix form for a mechanism, which consists of a planar four-bar linkage and an additional revolute joint connecting the four-bar linkage to the base. The flexibility of the mechanism is considered to provide additional conditions for solving the forces acting on the mechanism as has been suggested in [5]. The method is based on the equilibrium conditions of the mechanism [6, 7]. Because the mechanism is overdetermined, there are more unknown forces than the number of force equations. The compatibility conditions of the mechanism, which relate the Cartesian deflections to the external wrench (force/moment) via the flexibility matrix of the mechanism and also the joint deflections to the joint wrenches via the joint flexibility, are introduced. Simulations of the mechanism under different external wrenches are performed within the working range of the mechanism and the required driving torques are plotted for two cases.

2. Static Force Analysis

In this section, the static force equations of the mechanism shown in Figure 1(a) are given. This mechanism consists of a planar parallelogram linkage and a link that connects the parallelogram to the base with a revolute joint. The motion of the mechanism resembles the spatial four-bar (2R-2S) when its passive degree of freedom is actuated and the revolute joint pair, which provide the passive degree of freedom, is bifurcated [8]. In addition, the revolute joints, which would provide rotational freedom about the axes of links 3 and 4 (Figure 1(a)) are eliminated. The force equations are derived for each link and arranged for solving under given external loading.

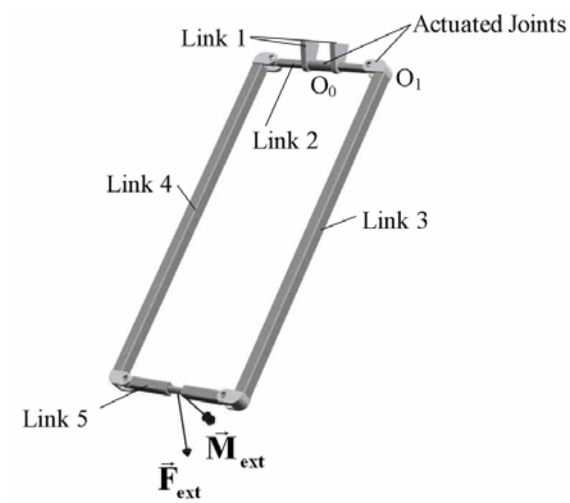

(a)

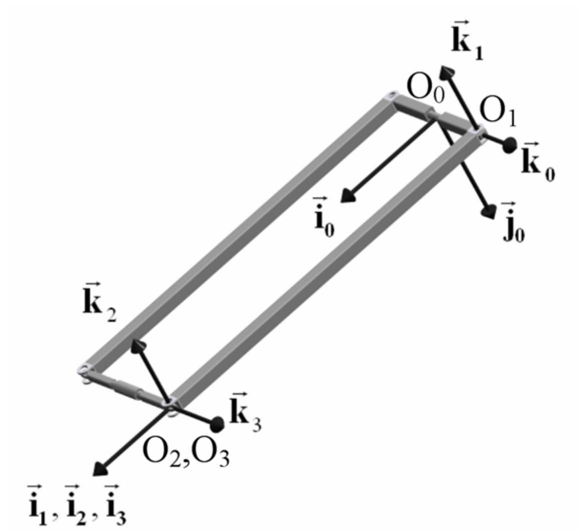

(b)

Figure 1(a) A simple mechanism which incorporates four-bar linkage, (b) Zero configuration of the mechanism.

The zero configuration indicating reference frames 0, 1, 2 and 3 attached to links 1, 2, 3, and 5 are shown in Figure 1(b). The Denavit-Hartenberg parameters [9] of the mechanism are listed in Table 2 where θ_i and d_i correspond to the rotation and translation about $\vec{k}_{i-1}$, and a_i and α_i represent the effective link length and twist angle about $\vec{i}_i$, respectively.

Additional reference frames are employed to formulate the motion of link 4 relative to link 2 (frame 5), and link 5 relative to link 4 (frame 4). The relative joint angles between these reference frames are the same as angles θ_1 and θ_3, respectively, due to the usage of the parallelogram mechanism. Detailed kinematic analysis of this mechanism is reported in [10].

Table 2 Denavit-Hartenberg parameters.

Link	θ_i	d_i (m)	a_i (m)	α_i
2	θ_1	$d_1 = 0.152$	0	$\pi/2$
3	θ_2	0	$a_2 = 0.610$	0
5	θ_3	0	0	$-\pi/2$

The kinematic and static force equations of the mechanism can be modelled by using the parameters in Table 2. Static force equations are obtained by considering the free-body diagrams of each link, which are shown in Figures 2(a) - (d) respectively. The force equation for link i, i = 2, ..., 5 is formulated as:

$$m_i\,\vec{\boldsymbol{g}} + \sum \vec{\boldsymbol{F}}_{\boldsymbol{ji}} = \boldsymbol{0} \tag{3}$$

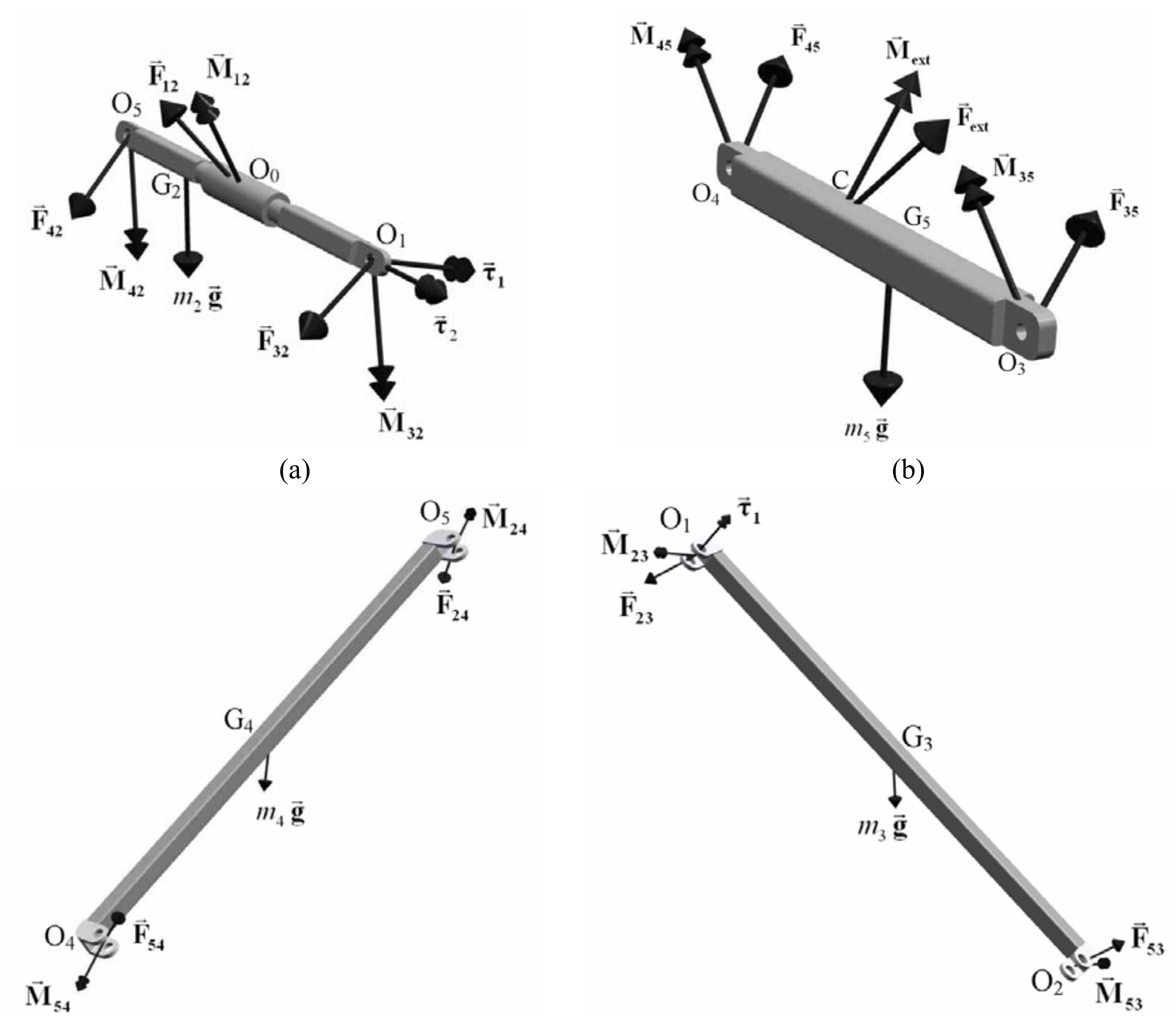

(c) (d)

Figure 2Free-body diagrams of (a) link 2, (b) link 5, (c) link 4, and (d) link 3.

and the moment equation about the mass center of the link is:

$$\sum \vec{\boldsymbol{r}}_{\boldsymbol{j}} \times \vec{\boldsymbol{F}}_{\boldsymbol{ji}} + \sum \vec{\boldsymbol{M}}_{\boldsymbol{ji}} = \boldsymbol{0} \tag{4}$$

The set of static force/moment equations of the mechanism can be obtained in the form of equations (3) and (4) after resolving the force/moment equations into the body frames of each link respectively.

$$\boldsymbol{T}\boldsymbol{W} = \boldsymbol{W}_{\boldsymbol{ext}} + \boldsymbol{W}_{\boldsymbol{g}} \tag{5}$$

where the term $\boldsymbol{T}$ on the left-hand side of the equation is a 24×27 transformation matrix formulated as:

$$\boldsymbol{T} = \begin{bmatrix} \boldsymbol{T}_{\boldsymbol{m}}^{(3,2)} & \boldsymbol{T}_{\boldsymbol{m}}^{(3,3)} & \boldsymbol{0} & \boldsymbol{0} & \boldsymbol{0} \\ \boldsymbol{0} & \boldsymbol{T}_{\boldsymbol{m}}^{(4,3)} & \boldsymbol{T}_{\boldsymbol{m}}^{(4,4)} & \boldsymbol{0} & \boldsymbol{0} \\ \boldsymbol{T}_{\boldsymbol{m}}^{(2,2)} & \boldsymbol{0} & \boldsymbol{0} & \boldsymbol{T}_{\boldsymbol{m}}^{(2,1)} & \boldsymbol{0} \\ \boldsymbol{0} & \boldsymbol{0} & \boldsymbol{T}_{\boldsymbol{m}}^{(1,4)} & \boldsymbol{T}_{\boldsymbol{m}}^{(1,1)} & \boldsymbol{T}_{\boldsymbol{m}}^{(1,0)} \end{bmatrix} \tag{6}$$

and the submatrices $\boldsymbol{T}_{\boldsymbol{m}}^{(i,j)}$ are based on the screw (adjoint) transformations which transform a given wrench in frame j to frame i given as:

$$\boldsymbol{T}_{\boldsymbol{m}}^{(i,j)} = \begin{bmatrix} \boldsymbol{R}^{(i,j)} & \boldsymbol{0} \\ \tilde{\boldsymbol{r}}_{O_iO_j}\, \boldsymbol{R}^{(i,j)} & \boldsymbol{R}^{(i,j)} \end{bmatrix} \tag{7}$$

and $\boldsymbol{T}_{\boldsymbol{m}}^{(i,i)}$ corresponds to a matrix of dimension 6×6 which is used to transform a wrench acting in one point to another point in the same reference frame i, $\boldsymbol{R}^{(i,j)}$ is the 3×3 rotation matrix from frame i to frame j, and $\tilde{\boldsymbol{r}}_{O_iO_j}$ is the skew symmetric matrix of the position vector defining origin of frame j with respect to frame i. The transformation matrix of equation (7) is used for the reaction wrenches of the actuated joints, and for the passive joints. The column of the transformation matrix corresponding to the axis of a passive joint is deleted because the moment about the passive revolute joint axis becomes zero.

In equation (5), the term $\boldsymbol{W}$ contains the reaction wrenches and driving torques and is given as:

$$\boldsymbol{W} = \left[\left(\boldsymbol{W}_{\boldsymbol{35}}^{(2)}\right)^T \quad \left(\boldsymbol{W}_{\boldsymbol{45}}^{(3)}\right)^T \quad \left(\boldsymbol{W}_{\boldsymbol{24}}^{(4)}\right)^T \quad \left(\boldsymbol{W}_{\boldsymbol{23}}^{(1)}\right)^T \quad \left(\boldsymbol{W}_{\boldsymbol{12}}^{(0)}\right)^T \right]^T \tag{8}$$

where $\boldsymbol{W}_{\boldsymbol{ij}}^{(k)}$ represents the wrench acting by link i on link j, expressed in reference frame k. For the reaction wrenches due to passive revolute joints, because the moment about the joint axis causes the rotation of the joint, hence there is no reaction moment about the joint axis and $\boldsymbol{W}_{ij}^{(k)}$ has the following form:

$$\boldsymbol{W}_{ij}^{(k)} = \left[\left(\boldsymbol{F}_{ij}^{(k)}\right)^T \quad \left(\boldsymbol{M}_{ij}^{(k)}\right)^T \right]^T = \left[F_{ij_x} \quad F_{ij_y} \quad F_{ij_z} \quad M_{ij_x} \quad M_{ij_y} \right]^T \tag{9}$$

and for the active revolute joints m, m = 1, 2, the joint torques can be combined with the reaction wrenches as:

$$\boldsymbol{W}_{ij}^{(k)} = \left[\left(\boldsymbol{F}_{ij}^{(k)}\right)^T \quad \left(\boldsymbol{M}_{ij}^{(k)}\right)^T \right]^T = \left[F_{ij_x} \quad F_{ij_y} \quad F_{ij_z} \quad M_{ij_x} \quad M_{ij_y} \quad \tau_m \right]^T \tag{10}$$

In equation (5), the term $\boldsymbol{W}_{\mathbf{ext}}$ is because of the external wrench acting on link 5 of the mechanism resolved into the body frames for each link due to the reaction forces, and is given as:

$$\boldsymbol{W}_{ext} = \left[\left(\boldsymbol{T}_m^{(3,3)} \left[\boldsymbol{F}_{ext}{}^T \quad \boldsymbol{M}_{ext}{}^T \right]^T \right) \quad \boldsymbol{0} \quad \boldsymbol{0} \quad \boldsymbol{0} \right]^T \tag{11}$$

The second term on the right-hand side of equation (5), $\boldsymbol{W}_{\boldsymbol{g}}$, includes the gravity forces acting on the mass center of each link, which are constant in the fixed frame, resolved into the body frames of the links:

$$\boldsymbol{W}_g = \left[\left(\boldsymbol{T}_m^{(3,0)} \left[m_5\, \boldsymbol{g}^T \quad \boldsymbol{0}^T \right]^T \right) \quad \left(\boldsymbol{T}_m^{(4,0)} \left[m_4\, \boldsymbol{g}^T \quad \boldsymbol{0}^T \right]^T \right) \quad \left(\boldsymbol{T}_m^{(2,0)} \left[m_3\, \boldsymbol{g}^T \quad \boldsymbol{0}^T \right]^T \right) \quad \left(\boldsymbol{T}_m^{(1,0)} \left[m_2\, \boldsymbol{g}^T \quad \boldsymbol{0}^T \right]^T \right) \right]^T \tag{12}$$

Equation (5) is overdetermined, i.e., there are more unknown forces/moments than the number of equations. To solve for the unknown forces/moments, the flexibility of the links and joints could be taken into account to formulate the force-deflection relations (known as the compatibility equations). Then, equation (5) combined with these compatibility equations can be solved by matrix inversion. While this solution can be performed based on the Jordan elimination techniques, or other numerically efficient methods, a modified matrix force method is used.

Equation (5) is decomposed into force and moment equations, then one of the forces is chosen as the independent force, and the other reaction forces and moments are written in terms of the independent force. The resultant set of equations reduces from 24 to 12 equations for 15 unknowns. The difference between the number of unknowns and the number of equations is three. The three unknowns will be referred to as "redundant forces/moments" in the following sections. This reduction also facilitates selection of the flexible members of the mechanism in the next section when solving for the forces. It should be noted that the reduction could affect the flexibility matrix of the mechanism since the reduction of the number of unknowns also reduces the flexibility matrix of the link and some of the coupling terms which relate the unknown forces/moments to the deflection of the links. Choosing $\boldsymbol{F}_{35}^{(2)}$ as the independent force to be kept, the other forces can be determined as:

$$\boldsymbol{F}_{45} = -\boldsymbol{R}^{(3,2)}\,\boldsymbol{F}_{35}^{(2)} - m_5\,\boldsymbol{R}^{(3,0)}\,\boldsymbol{g}^{(0)} - \boldsymbol{F}_{ext}^{(3)} \tag{13}$$

$$\boldsymbol{F}_{24} = -\boldsymbol{R}^{(4,2)}\,\boldsymbol{F}_{35}^{(2)} - (m_4 + m_5)\boldsymbol{R}^{(4,0)}\,\boldsymbol{g}^{(0)} - \boldsymbol{R}^{(4,3)}\,\boldsymbol{F}_{ext}^{(3)} \tag{14}$$

$$\boldsymbol{F}_{23} = \boldsymbol{R}^{(1,2)}\,\boldsymbol{F}_{35}^{(2)} - m_3\,\boldsymbol{R}^{(1,0)}\,\boldsymbol{g}^{(0)} \tag{15}$$

$$\boldsymbol{F}_{12} = -\boldsymbol{R}^{(0,3)}\,\boldsymbol{F}_{ext}^{(3)} - \sum_{i=2}^{5} m_i\,\boldsymbol{g}^{(0)} \tag{16}$$

The static equation of the mechanism reduces to the following form:

$$\boldsymbol{J}^{\boldsymbol{u}}\,\boldsymbol{u} = \boldsymbol{J}_{ext}^{\boldsymbol{u}}\,\boldsymbol{W}_{ext} + \sum_{i=2}^{5}\left(\boldsymbol{J}_{g}^{\boldsymbol{u}}\,\boldsymbol{F}_{g}\right)_i \tag{17}$$

where the term on the left-hand side of equation (17) includes the unknown forces/moments and driving torques, the first term on the right-hand side is the effort of the external wrench on the mechanism and the second term is the effect of the gravity on the mechanism. The terms in equation (17) are given as:

$$\boldsymbol{u} = \left[\left(\boldsymbol{W}_{35}^{(2)}\right)^T \quad \left(\boldsymbol{M}_{45}^{(3)}\right)^T \quad \left(\boldsymbol{M}_{24}^{(4)}\right)^T \quad \left(\boldsymbol{M}_{23}^{(1)}\right)^T \quad \left(\boldsymbol{M}_{12}^{(0)}\right)^T\right]^T \tag{18}$$

where $\boldsymbol{u}$ is a 15×1 vector whose components are defined in equations (8) through (10);

$$\boldsymbol{J}^{\boldsymbol{u}} = \begin{bmatrix} \tilde{\boldsymbol{r}}_{O_4O_2}\,\boldsymbol{R}^{(3,2)} & \boldsymbol{R}_2^{(3,2)} & \boldsymbol{I}_2 & \boldsymbol{0} & \boldsymbol{0} & \boldsymbol{0} \\ \tilde{\boldsymbol{r}}_{O_5O_4}\,\boldsymbol{R}^{(4,2)} & \boldsymbol{0} & -\boldsymbol{R}_2^{(4,3)} & \boldsymbol{I}_2 & \boldsymbol{0} & \boldsymbol{0} \\ \tilde{\boldsymbol{r}}_{O_2O_1} & -\boldsymbol{I}_2 & \boldsymbol{0} & \boldsymbol{0} & \boldsymbol{R}^{(2,1)} & \boldsymbol{0} \\ -\tilde{\boldsymbol{r}}_{O_5O_1}\,\boldsymbol{R}^{(1,2)} & \boldsymbol{0} & \boldsymbol{0} & -\boldsymbol{R}_2^{(1,4)} & -\boldsymbol{I} & \boldsymbol{R}^{(1,0)} \end{bmatrix} \tag{19}$$

Matrices $\boldsymbol{I}$ and $\boldsymbol{I}_2$ are 3×3 and 3×2 identity matrices, where a column of $\boldsymbol{I}_2$ corresponding to a passive joint is deleted. Matrix $\boldsymbol{R}_2^{(i,j)}$ is the rotation matrix from frame i to frame j with the column corresponding to the passive joint freedom deleted. The expressions for matrices $\boldsymbol{J}_{ext}^{\boldsymbol{u}}$, $\boldsymbol{J}_{g_i}^{u}$, $i = 2, \ldots, 5$, can be calculated as:

$$\boldsymbol{J}_{ext}^{\boldsymbol{u}} = \begin{bmatrix} \tilde{\boldsymbol{r}}_{CO_4} & -\boldsymbol{I} \\ -\tilde{\boldsymbol{r}}_{O_5O_4}\,\boldsymbol{R}^{(4,3)} & \boldsymbol{0} \\ \boldsymbol{0} & \boldsymbol{0} \\ -\tilde{\boldsymbol{r}}_{O_5O_0}\,\boldsymbol{R}^{(1,3)} & \boldsymbol{0} \end{bmatrix} \tag{20}$$

$$\boldsymbol{J}_{g_2}^{\boldsymbol{u}} = \left[\boldsymbol{0} \quad \boldsymbol{0} \quad \boldsymbol{0} \quad \left(\tilde{\boldsymbol{r}}_{G_2O_0}\,\boldsymbol{R}^{(1,0)}\right)^T\right]^T \tag{21}$$

$$\boldsymbol{J}_{g_3}^{\boldsymbol{u}} = \left[\boldsymbol{0} \quad \boldsymbol{0} \quad \left(\tilde{\boldsymbol{r}}_{G_3O_1}\,\boldsymbol{R}^{(2,0)}\right)^T \quad \left(\tilde{\boldsymbol{r}}_{O_0O_1}\,\boldsymbol{R}^{(1,0)}\right)^T\right]^T \tag{22}$$

$$\boldsymbol{J}_{g4}^{\boldsymbol{u}} = \left[\boldsymbol{0} \quad \left(\tilde{\boldsymbol{r}}_{G_4\boldsymbol{O}_5}\,\boldsymbol{R}^{(4,0)}\right)^{\boldsymbol{T}} \quad \boldsymbol{0} \quad \left(\tilde{\boldsymbol{r}}_{\boldsymbol{O_0 O}_5}\,\boldsymbol{R}^{(1,0)}\right)^{\boldsymbol{T}}\right]^T \tag{23}$$

$$\boldsymbol{J}_{g5}^{\boldsymbol{u}} = \left[\left(\tilde{\boldsymbol{r}}_{G_5\boldsymbol{O}_4}\,\boldsymbol{R}^{(3,0)}\right)^{\boldsymbol{T}} \quad \left(-\tilde{\boldsymbol{r}}_{\boldsymbol{O}_5\boldsymbol{O}_4}\,\boldsymbol{R}^{(4,0)}\right)^{\boldsymbol{T}} \quad \boldsymbol{0} \quad \left(\tilde{\boldsymbol{r}}_{\boldsymbol{O_0 O}_5}\,\boldsymbol{R}^{(1,0)}\right)^{\boldsymbol{T}}\right]^T \tag{24}$$

where $\tilde{\boldsymbol{r}}_{G_iO_j}$ is the skew symmetric matrix of the mass center position of link i with respect to the origin of the reference frame j, and $\tilde{\boldsymbol{r}}_{CO_4}$ corresponds to the position of the point of application of the external wrench, point C, relative to the origin of the coordinate frame 4, which can be seen in Figure 2.

The dimensions of the gravity related Jacobians $\boldsymbol{J}_{g\,i}^{u}$, are 12×3 whereas the dimension of the Jacobian related to the external force, $\boldsymbol{J}_{\boldsymbol{ext}}^{\boldsymbol{u}}$, is 12×6. The static force equation (17) can be solved by considering the flexibility of the mechanism, which is discussed in Section 3.

3. Solution of Forces

In this section the flexibility of the mechanism is considered first as the solution method is based on the flexibility matrix of the mechanism. The links of the mechanism are modelled as the beams and the flexibility matrix of the beams can be found in the literature [6]. The compatibility conditions, formulated as three equations, are used to solve for the three redundant forces/moments, by means of which three additional virtual freedoms are introduced. The redundant forces/moments are chosen so that equation (17) can be written in the following form by grouping the remaining unknown forces/moments together (known as the primary structure), denoted by $\boldsymbol{u}_p$, and the redundant forces/moments together (known as the secondary structure), denoted by $\boldsymbol{u}_s$, as:

$$\boldsymbol{J}_{\boldsymbol{p}}^{\boldsymbol{u}}\,\boldsymbol{u}_p = \boldsymbol{J}_{\boldsymbol{ext}}^{\boldsymbol{u}}\,\boldsymbol{W}_{\boldsymbol{ext}} + \sum_{i=2}^{5}\left(\boldsymbol{J}_g^{u}\,\boldsymbol{F}_g\right)_i - \boldsymbol{J}_s^{\boldsymbol{u}}\,\boldsymbol{u}_s \tag{25}$$

where $\boldsymbol{J}^{\boldsymbol{u}} = \left[\boldsymbol{J}_{\boldsymbol{p}}^{\boldsymbol{u}} \quad \boldsymbol{J}_s^{\boldsymbol{u}}\right]$.

Once the redundant forces/moments are calculated from the compatibility conditions, the statically determined forces can be solved directly from equation (25). The choice of redundant forces is made such that the flexibility matrix corresponding to the redundant forces is diagonal, or as close to diagonal as possible, because choosing a diagonal matrix reduces the possibility of the flexibility matrix related to the redundant forces being ill conditioned. The flexibility matrix of the primary structure is formulated by using the flexibility of the links and the actuated joints. The reaction moments between the base and link 2 are excluded from equation (25) since generally it is not necessary to calculate them [3, 4]. Thus, equation (25) is reduced into 10 equations for 13 unknowns.

The flexibility equation for each of the links is given by:

$$\boldsymbol{\delta}^{(k)} = \boldsymbol{c}_i\,\boldsymbol{W}^{(k)} \tag{26}$$

where $\boldsymbol{\delta}^{(k)}$ is the deflection of the link in the coordinate frame k, $\boldsymbol{c}_i$ is the compliance matrix of link i and $\boldsymbol{W}^{(k)}$ is the reaction wrench of the link. This equation can be used in obtaining the compliance matrix of each link under the reaction forces.

The flexibility matrices of the links, modelled as beams, are taken from [6]. After rearranging, the resultant flexibility matrix for the secondary structure is given as:

$$\boldsymbol{C}_s = diag\begin{pmatrix} \frac{a_2}{GJ_3} & \frac{d_5}{GJ_5} & \frac{a_4}{GJ_4} \end{pmatrix} \tag{27}$$

where d_5 is the length of link 5 which is twice the length of d_1, G is the shear modulus of elasticity, J_i is the polar moment of inertia of link i._The diagonal entries of $\boldsymbol{C}_s$ correspond to the redundant moments chosen as $M_{35_x}^{(2)}$, $M_{45_z}^{(3)}$, and $M_{24_x}^{(4)}$. The flexibility matrix for the primary structure denoted by $\boldsymbol{C_p}$, which is a 10×10 matrix, is in the following form:

$$\boldsymbol{C}_p = diag\begin{pmatrix}\boldsymbol{c_3} & \boldsymbol{c_5} & \boldsymbol{c}_4 & \boldsymbol{c}_2 & c_{m1} & c_{m2}\end{pmatrix} \tag{28}$$

where c_{mi} is the compliance of actuated joint i [11], and the compliance matrix $\boldsymbol{c}_i$ of link i, i = 2, …, 5, are:

$$\boldsymbol{c}_2 = diag\begin{pmatrix}\dfrac{2d_1}{EI_x} & \dfrac{2d_1}{EI_y}\end{pmatrix} \tag{29}$$

$$\boldsymbol{c_3} = \begin{bmatrix} \dfrac{a_2}{A_2 E} & 0 & 0 & 0 \\ 0 & \dfrac{a_2^3}{3EI_z} & 0 & 0 \\ 0 & 0 & \dfrac{a_2^3}{3EI_y} & -\dfrac{a_2^3}{2EI_y} \\ 0 & 0 & -\dfrac{a_2^3}{2EI_y} & \dfrac{a_2^3}{EI_y} \end{bmatrix} \tag{30}$$

$$c_4 = \frac{a_4}{EI_y} \tag{31}$$

$$c_5 = \frac{d_5}{E\,I_y} \tag{32}$$

and E is the Young's modulus of elasticity, A_i is the cross-sectional area of link i, and I_x, I_y, I_z are the moments of inertia of the corresponding link about the principal axes of the link.

The total strain energy of the mechanism can be written in the following form:

$$U = \frac{1}{2}\boldsymbol{u_p}^T\boldsymbol{\delta}_p + \frac{1}{2}\boldsymbol{u_s}^T\boldsymbol{\delta}_s \tag{33}$$

where $\boldsymbol{\delta}_p$ and $\boldsymbol{\delta}_s$ are respectively the 10×1 and 3×1 infinitesimal displacement vectors of the primary and secondary structures expressed in the body coordinate frames for the link, where $\boldsymbol{\delta}_s$ includes torsional deflections of links 3, 4 and 5 about their axes. The compliance matrix of the primary structure (and secondary structure) that relates the forces acting on the links to the infinitesimal displacements has the following form:

$$\boldsymbol{\delta} = \boldsymbol{C}\,\boldsymbol{u} \tag{34}$$

Substituting equation (34) in equation (33), the strain energy of the mechanism could be calculated as:

$$U = \frac{1}{2}\boldsymbol{u_p}^T\boldsymbol{C}_p\boldsymbol{u_p} + \frac{1}{2}\boldsymbol{u_s}^T\boldsymbol{C}_s\,\boldsymbol{u_s} \tag{35}$$

The strain energy can be written in terms of external wrenches, gravity forces and redundant internal moments by substituting equation (25) for $\boldsymbol{u}_p$ in equation (35). By differentiating equation (35) with respect to these forces/moments, it is possible to obtain a relation between the infinitesimal displacements corresponding to the external wrench and the infinitesimal displacement corresponding to the secondary structure as:

$$\begin{bmatrix} \boldsymbol{\Delta} \\ \boldsymbol{\delta}_s \end{bmatrix} = \begin{bmatrix} \boldsymbol{c}_{11} & \boldsymbol{c}_{12} \\ \boldsymbol{c}_{21} & \boldsymbol{c}_{22} \end{bmatrix} \begin{bmatrix} \boldsymbol{W}_{ext} \\ \boldsymbol{u}_s \end{bmatrix} + \sum_{k=2}^{5} \left(\begin{bmatrix} \boldsymbol{c}_{gp} \\ \boldsymbol{c}_{gs} \end{bmatrix} \boldsymbol{F}_g \right)_k \tag{36}$$

where $\boldsymbol{\Delta}$ is the infinitesimal displacement of the mechanism under the external wrench $\boldsymbol{W}_{ext}$ in the fixed frame while $\boldsymbol{\delta_s}$ includes the deflection of the secondary mechanism, corresponding to $M^{(2)}_{35_x}$, $M^{(3)}_{45_z}$, and $M^{(4)}_{24_x}$, expressed in the body coordinate frames of links 3, 5, and 4, respectively. The submatrices $\boldsymbol{c}_{ij}$, i = 1, 2 and j = 1, 2, and $\boldsymbol{c}_{gpk}$, and c_{gsk} k = 2, …, 5, are calculated as:

$$\boldsymbol{c}_{11} = \boldsymbol{J}^{\boldsymbol{u}\,\boldsymbol{T}}_{\boldsymbol{ext}} \boldsymbol{C}_p \boldsymbol{J}^{\boldsymbol{u}}_{\boldsymbol{ext}} \tag{37}$$

$$\boldsymbol{c}_{12} = -\frac{1}{2} \boldsymbol{J}^{\boldsymbol{u}\,\boldsymbol{T}}_{\boldsymbol{ext}} \boldsymbol{C}_p \boldsymbol{J}^{\boldsymbol{u}}_s \tag{38}$$

$$\boldsymbol{c}_{21} = -\frac{1}{2} \boldsymbol{J}^{\boldsymbol{u}\boldsymbol{T}}_s \boldsymbol{C}_p \boldsymbol{J}^{\boldsymbol{u}}_{ext} \tag{39}$$

$$\boldsymbol{c}_{22} = \boldsymbol{J}^{\boldsymbol{u}\boldsymbol{T}}_s \boldsymbol{C}_p \boldsymbol{J}^{\boldsymbol{u}}_s + \boldsymbol{C}_s \tag{40}$$

$$\left(\boldsymbol{c}_{gp}\right)_k = \left(\boldsymbol{J}^{\boldsymbol{u}}_{\boldsymbol{ext}}\right)^T \boldsymbol{C}_p \left(\boldsymbol{J}^{\boldsymbol{u}}_{\boldsymbol{g}}\right)_k \tag{41}$$

$$\left(\boldsymbol{c}_{gs}\right)_k = \left(\boldsymbol{J}^{\boldsymbol{u}}_s\right)^T \boldsymbol{C}_p \left(\boldsymbol{J}^{\boldsymbol{u}}_{\boldsymbol{g}}\right)_k \tag{42}$$

The first term on the right-hand side of equation (36) is the flexibility of the mechanism due to external loading and the redundant moments while the second term provides additional flexibility due to the gravity forces acting on the mechanism [12]. Calculating the compliance matrices, the redundant forces/moments can be solved by using the compatibility equation (lower part of equation (36) which corresponds to the twisting moments of links 3, 4 and 5) when the deflections of the secondary structure are set to zero, i.e., $\boldsymbol{\delta}_s = 0$ [6]:

$$\boldsymbol{u_s} = -\boldsymbol{c}_{22}^{-1} \left(\boldsymbol{c}_{21} \boldsymbol{W}_{\boldsymbol{ext}} + \sum_{k=2}^{5} \left(\boldsymbol{c}_{gs} \boldsymbol{F}_{\boldsymbol{g}} \right)_k \right) \tag{43}$$

and the remaining forces and driving torques can be found by using equation (25). It is worth mentioning that the formulated compliance matrix of the mechanism using the structural matrix force and stiffness methods has similar form to the one derived in [12], while in [12] only the actuator flexibilities of a parallel manipulator are modelled (and the link flexibilities are neglected) and the gravitational and reaction forces/moments are included.

4. Simulation Results

The simulation of the mechanism is performed to solve for the driving torques within the working range of the mechanism, i.e., for $0^0 < \theta_1 < 360^o$ and $-90^0 < \theta_2 < 90^o$. The links are considered as hollow steel tubes with rectangular cross sections (density of 7800 kg/m^3, $E = 1.903\cdot10^{11}$ Pa, $G = 7.309\cdot10^{10}$ Pa). The simulation results are given in Figures 3 and 4, for a zero external wrench and a nonzero external wrench of $\boldsymbol{W}_{ext} = [23 \quad 13.1 \quad 13.1 \quad 4 \quad 6 \quad 6]$ in the body coordinate frame of link 5, respectively. A step size of 4^o and 1^o are used for θ_1 and θ_2, respectively. Very high driving torques are observed along $\theta_2 = \pm 90^\circ$ which correspond to the singularity of the parallelogram. For illustration purposes, these high values are not shown in the contour plots of Figures 3 and 4.

In Figure 3, which corresponds to zero external wrench, the plot of driving force indicates symmetry due to the symmetric configuration of the mechanism. In this figure, the maximum torques for the base motor (links 2) are at around (θ_1, θ_2) = (90˚, 0˚) and (270˚, 0˚), and for the motor which actuates link 3 (the parallelogram mechanism) are around (θ_1, θ_2) = (0˚, ±90˚) and (180˚, ±90˚). In Figure 4, which corresponds to nonzero external wrench, the maximum torques are at (270˚, 0˚) for the base motor and (0˚, ±90˚) for the motor which actuates the parallelogram mechanism. The largest driving torques occur at the positions when the gravity forces create the maximum moment about the axis of the corresponding actuated joint in the case of zero external force (Figure 3). The plot of the driving torques look different in the case of an external wrench, however, the maximum driving torques occur in the same positions as that of the zero gravity case.

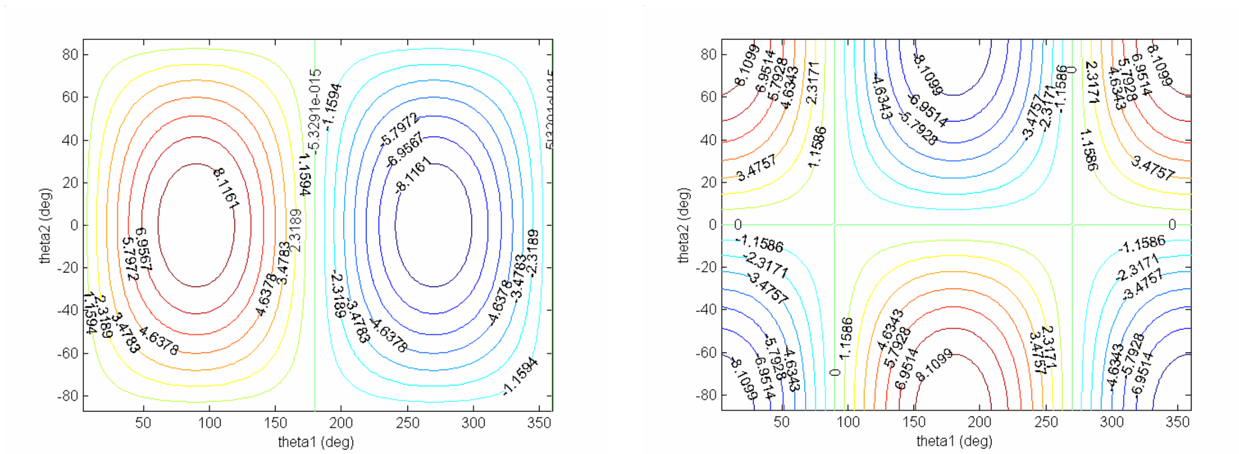

(a) (b)

Figure 3 Simulation results: The driving torque for (a) the base joint, (b) the parallelogram mechanism.

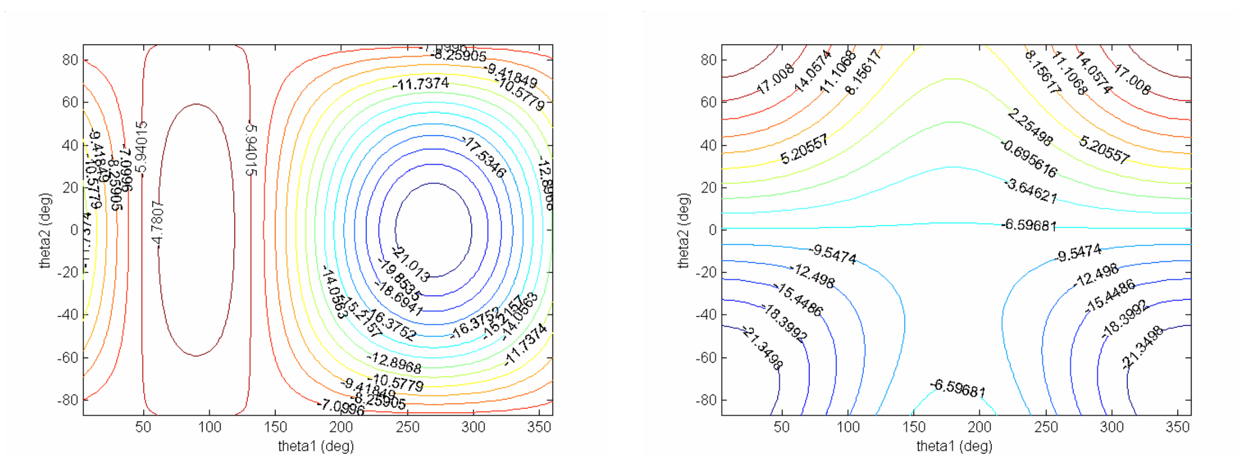

(a) (b)

Figure 4 Simulation results: The driving torques for (a) the base joint (b) the parallelogram mechanism.

The simulation results are verified by using the pseudoinverse solution of equation (5) to calculate the minimum norm solution of joint torques for a given external wrenches, which is frequently used in robotics for redundant manipulators. Specifically, the weighted generalized pseudoinverse, which is based on the minimum strain energy for the mechanism, is considered using the following formula:

$$\text{Minimize } \frac{1}{2}\boldsymbol{\delta}^T \boldsymbol{u} \qquad \text{subjected to} \qquad \boldsymbol{J}^u \boldsymbol{u} = \boldsymbol{W}_k \tag{44}$$

where $\boldsymbol{W_k}$ includes the effect of gravity and external wrench. The weighted right pseudoinverse solution employing the compliance matrix of the mechanism in joint space is obtained as in [13]:

$$\boldsymbol{u} = \boldsymbol{J}^{\#}\boldsymbol{W}_{\mathrm{k}} \tag{45}$$

and

$$\boldsymbol{J}^{\#} = \boldsymbol{C}^{-1}\left(\boldsymbol{J}^{u}\right)^{T}\left(\boldsymbol{J}^{u}\,\boldsymbol{C}\left(\boldsymbol{J}^{u}\right)^{T}\right)^{-1} \tag{46}$$

The solution given in equation (45) is the particular solution for the given external wrench and is simulated under the same conditions as of the matrix force method. The same results for the driving torques as in Figures 3 and 4 are obtained. This result is specific to this mechanism, as the internal forces are also checked for both methods. The internal forces/moments for two poses of ((θ_1, θ_2) = (90º,0) and (45º,45º)), for the case of zero external wrench are listed in Table 3. As can be seen from Table 3, while the driving torques are the same, the reaction forces/moments differ from each other. This is an expected result since the solution of the optimized generalized inverse depends on the metric used to solve the problem while the matrix force method relies on the compatibility equations.

*Table 3 Driving Torques and Internal Forces/Moments at two different positions (**W_{ext}** = **0**)*

		Matrix Force Method		Weighted Generalized Pseudoinverse	
		(θ_1,θ_2) = (90º,0)	(θ_1,θ_2) = (45º,45º)	(θ_1,θ_2) = (90º,0)	(θ_1,θ_2) = (45º,45º)
Driving Torques (Nm)	τ_1	0	4.641	0	4.641
	τ_2	9.281	4.641	9.281	4.641
Internal Forces (N) and Moments (Nm) for Secondary Structure and Primary Structure	$M_{35_x}^{(2)}$	−0.409	−0.398	−0.59	−0.414
	$M_{45_z}^{(3)}$	0.845	0.478	0.202	0.438
	$M_{24_x}^{(4)}$	−0.218	0.1	−0.635	0.1146
	$F_{35_x}^{(2)}$	0	2.759	0	2.759
	$F_{35_y}^{(2)}$	0	4.854	0	4.854
	$F_{35_z}^{(2)}$	0.688	−0.10	1.923	−0.09
	$M_{35_y}^{(2)}$	−0.845	−0.278	−0.203	−0.205
	$M_{45_x}^{(3)}$	−0.440	−0.336	−0.635	−0.276
	$M_{24_y}^{(4)}$	7.181	4.6996	7.293	4.634
	$M_{23_x}^{(1)}$	−0.409	−1.809	−0.590	−1.868
	$M_{23_y}^{(1)}$	2.099	1.247	1.989	1.282

Conclusion

In this article, the static force analysis of a mechanism, which incorporates a four-bar linkage, is formulated. The mechanism is overdetermined due to the spatial loading acting on it. To solve for the reaction forces and driving torques, the flexibility of the mechanism is considered. From the strain energy equation of the mechanism, the flexibility matrices, which relate the deflection of the mechanism and the deflection of the secondary structure to the external wrench, redundant forces/moments and the gravity forces, are derived and are used to solve for the redundant forces/moments. Then the static force equations for the primary mechanism are used to find the driving torques. The simulations are performed to estimate the driving torques necessary for the mechanism for different external loading. The verification of the simulations is performed by employing the particular solution of the generalized weighted pseudoinverses.

References

1. Mroz, G., and Notash, L., Design and Prototype of Parallel, Wire-Actuated Robots with a Constraining Linkage, J. Robotic Systems, 21(12):677-687, 2004
2. Angeles, J., The Qualitative Synthesis of Parallel Manipulators, ASME Journal of Mechanical Design, 126:617-624, 2004
3. Shigley, J. E., and Uicker, J. J., Theory of Machines and Mechanisms, McGraw-Hill Int. Editions, 1995
4. Waldron, K. J., and Kinzel, G. L., Kinematics, Dynamics, and Design of Machinery, John Wiley & Sons, 2004
5. Bagci, C., Determining General and Overclosing Constraints in Mechanism Mobility Using Structural Finite Element Joint Freedoms, Transactions of the ASME, 114:376-383, 1992
6. Przemieniecki, J. S., Theory of Matrix Structural Analysis, Dover Publications, 1985
7. West, H. H., Fundamentals of Structural Analysis, John Wiley and Sons, 1993
8. Phillips, J., Freedom in Machinery, Introducing Screw Theory, Vol. 1, Cambridge University Press, 1984
9. Paul, R. P., Robot manipulators : mathematics, programming, and control ; the computer control of robot manipulators, M.I.T. Press, 1981
10. Sahin, S., and Notash, L., Kinematics, Workspace and Stiffness Analysis of Wire-Actuated Parallel Manipulators, Proc. of 11th World Congress in Mechanism and Machine Science, 5 pages, 2004
11. Asada, H., and Silotine, J.-J. E., Robot Analysis and Control, John Wiley and Sons Inc, 1986
12. Yi, B., and Freeman, R., Geometric Analysis of Antagonistic Stiffness in Redundantly Actuated Parallel Mechanisms, J. Robotic Systems, 10(5):581-603,1992
13. Patterson, T., and Lipkin, H., Duality of Constrained Elastic Manipulators, Proc. of IEEE International Conference on Robotics and Automation, 2820:2825, 1991